Electronic Supplementary Material (ESI) for Organic & Biomolecular Chemistry

Non-covalent duplex to duplex crosslinking of DNA in solution revealed by single molecule force spectroscopy

Benjamin D. Rackham, Lesley A. Howell, Andrew N. Round* and Mark Searcey*

Supporting Information

Atomic Force Microscopy (AFM) Crosslinking Analysis

AFM imaging was used to estimate the degree of crosslinking induced by intercalation for various intercalators, as described in the text. For representative populations of duplex DNA strands (n = 83-239) the proportion of DNA strands that were compact, coiled or crossed over was measured directly from the AFM images. Figure S1 shows that this proportion was higher for the bisacridine 1 sample than for the others considered. Table S1 reports the P-values for the comparisons of the datasets to each other, and shows that the proportion of compact, coiled and crossed-over DNA strands in the bisacridine 1 sample is significantly different from those for the echinomycin, 9-aminoacridine (a monointercalator sharing the same chromophore as bisacridine 1) and DNA-only control samples.

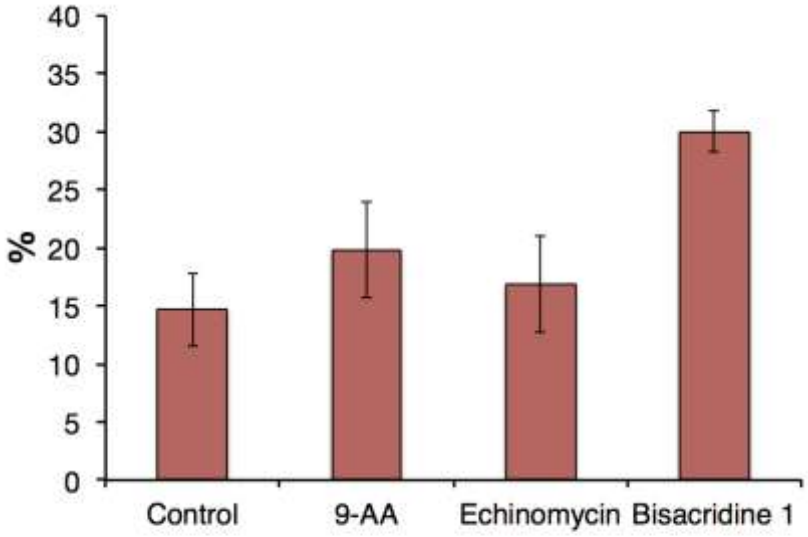

Figure S1. Proportion of compact, coiled and crossed-over DNA strands in samples containing no intercalator (control), monointercalator 9-aminoacridine (9-AA), echinomycin and bisacridine **1**. Error bars are 1 SD.

Table S1. P-values for unpaired t-tests (two-tailed)

	control	9-amino acridine	echino-mycin	bisacridine 1
control				
9-aminoacridine	0.2146			
echinomycin	0.5301	0.5515		
bisacridine 1	**0.0061 ****	**0.0249 ***	**0.021 ***	

Single Molecule Force Spectroscopy Analysis

Force spectroscopy data was first assessed within the JPK processing software. All single rupture events to which the extended freely jointed chain model (eFJC) [S1] could be fit were selected for further analysis. Where multiple events occurred in the same separation cycle, only the last event was considered. Free parameters in the eFJC model include contour length, breaking force and Kuhn length. The Kuhn length for a single polyethylene glycol (PEG) polymer (as we use here as a flexible spacer) has been estimated as 0.7 nm [S2]. Akhremitchev has shown [S3] that the Kuhn length is diagnostic for the presence of a single polymer stretch, since the value of the apparent Kuhn length varies as 1/n, where n = number of simultaneous parallel polymer stretches. Figure S2 shows plots of rupture force vs. Kuhn length for the crosslinking events mediated by the two bisacridines, echinomycin and TANDEM as used in this work. In each case, it can be seen that below a Kuhn length value of 0.6 nm there is an increase in the number of high force events, while there are also substantial populations of events with similar forces to the events where the Kuhn length exceeds 0.6 nm. Figure S3 shows that, at comparable loading rates, the stretches fit by Kuhn lengths of 0.6 nm or greater ruptured at lower forces than the stretches fit by Kuhn lengths lower than 0.6 nm. This result is in accordance with the predictions of Akhremitchev and suggests that events with lower Kuhn lengths represent multiple simultaneous (or nearly so) bond ruptures. We therefore selected for further analysis only those events with a Kuhn length of 0.6 nm or greater. Table 1 in the main text summarises the number of events fitting the eFJC model, and the number of events for which that fit produced a Kuhn length of 0.6 nm or greater.

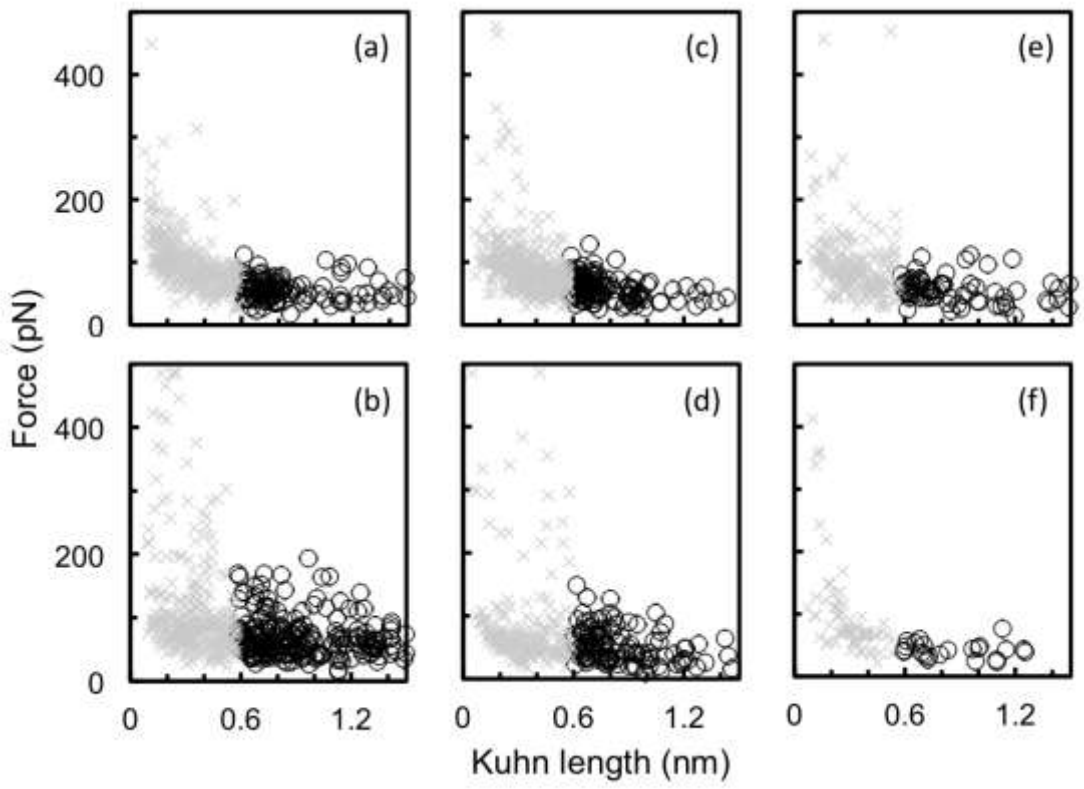

Figure S2. Plots of Kuhn length vs. rupture force for (a) bisacridine 1 crosslinking GC-terminated DNA, (b) bisacridine 1 / AT, (c) bisacridine 2 / GC, (d) bisacridine 2 / AT, (e) echinomycin / GC, and (f) TANDEM / AT. Crosses represent events fit by a Kuhn length less than 0.6 nm, open circles represent events fit by Kuhn lengths of 0.6 nm or greater.

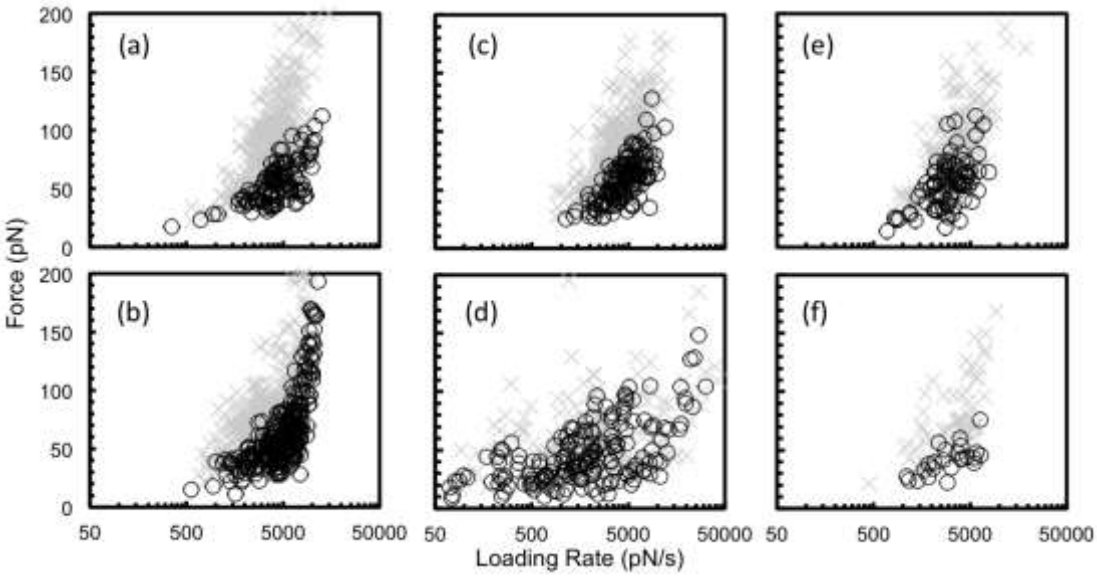

Figure S3. Plots of loading rate vs. rupture force for (a) bisacridine 1 crosslinking GC-terminated DNA, (b) bisacridine 1 / AT, (c) bisacridine 2 / GC, (d) bisacridine 2 / AT, (e)

echinomycin / GC, and (f) TANDEM / AT. Crosses represent events fit by a Kuhn length less than 0.6 nm, open circles represent events fit by Kuhn lengths of 0.6 nm or greater.

Dynamic Force Spectroscopy Analysis

The data selected by the above criteria was ordered by loading rate into bins of equal width and histograms of the rupture forces in each loading rate bin were fit by Gaussian distributions. The most probable rupture forces predicted by these Gaussian fits were then used to construct a dynamic force spectrum, as presented in figure 4(a) in the main text. This spectrum was then fit by the Friddle-Noy method [S4, S5] in order to extract values for the free parameters k_{off} and x_β (the intrinsic unbinding rate of the bond and the distance to the transition state, respectively) and, where sufficient data at low loading rates exists, a third parameter, the equilibrium force f_{eq} (the minimum force required to move the binding pair apart by the distance x_β, beyond which they can no longer instantaneously rebind). From f_{eq} may be obtained ΔG_u, the free energy of unbinding, for the bond. In one case (the interaction between bisacridine 2 and AT-terminated DNA) there was sufficient data to fit both the equilibrium and non-equilibrium regimes of the dynamic force spectrum, and in this case the data was fit to equation S1 [S4, S5] in OriginPro™ (OriginLab, ver. 8.0724):

$$\langle f \rangle \cong f_{eq} + f_\beta . ln\left(1 + e^{-\gamma} . \frac{r}{f_\beta . k_{u(f_{eq})}}\right) \quad \text{(S1)}$$

where <f> is the mean rupture force, $f_\beta = k_BT/x_\beta$ is the thermal force scale, k_BT is the Boltzmann constant multiplied by the temperature, $\gamma = 0.577\ldots$ is Euler's constant and r is the loading rate. Values of the parameters x_β, $k_{u(feq)}$ (the unbinding constant at f_{eq}) and f_{eq} were obtained from the fit of equation S1 to the data, while k_{off} was obtained from the value of $k_{u(feq)}$ and equation S2:

$$k_{off} = {k_{u(f_{eq})}} \Big/ exp\left[\frac{\left(f_{eq} - \frac{1}{2}k_{eff} . x_\beta\right)}{f_\beta}\right] \quad \text{(S2)}$$

where k_{eff} is the effective spring constant of the system comprising the cantilever stiffness k_c and the linker stiffness k_l; $k_{eff} = k_c.k_l/(k_c+k_l)$. A value of 150 Nm^{-1} was used for the linker stiffness [S2]. For the other datasets, insufficient data at low loading rates required that the data be fit with equation S3 [S4, S5], a high loading rate limit approximation of equation S1:

$$\langle f \rangle_{r\to\infty} \cong f_\beta . ln\left(e^{-\gamma} . \frac{r}{f_\beta . k_{off}}\right) \quad \text{(S3)}$$

where $\langle f \rangle_{r\to\infty}$ is the mean rupture force in the limit of high loading rate. Values of x_β and k_{off} were found from the fit of equation S2 to the data and presented in table 2 of the main text. Figure S4 shows the dynamic force spectra and fits to either equation S1 or equation S3 for all the crosslinking intercalation intercations studied in this work.

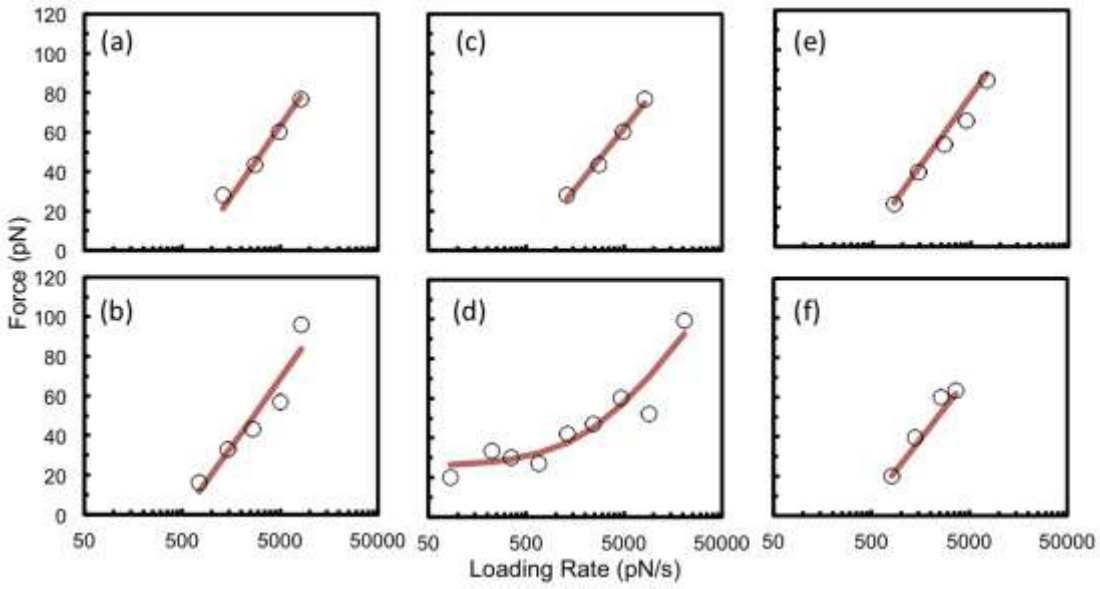

Figure S4. Dynamic force spectra with fits to the Friddle-Noy model for (a) bisacridine 1 crosslinking GC-terminated DNA, (b) bisacridine 1 / AT, (c) bisacridine 2 / GC, (d) bisacridine 2 / AT, (e) echinomycin / GC, and (f) TANDEM / AT. Open circles represent most probable rupture forces and loading rates from the data, and solid lines represent fits to either the full Friddle-Noy model (d) or the high loading rate limit model (a, b, c, e and f).

Finally, the validity of the Friddle-Noy model is demonstrated by the linear scaling relationship between the exponentials of the mean rupture force and loading rate according to equation S4 [S4]:

$$e^{-\gamma} . R(0) = e^{\langle f \rangle / f_\beta} - e^{f_{eq} / f_\beta}, \qquad R(0) = \frac{r}{f_\beta . k_{off}} \quad \text{(S4)}$$

Figure S5 shows that the data for the bisacridine 2 / AT interaction, for which we have the appropriate data, satisfies the criterion imposed by equation S4.

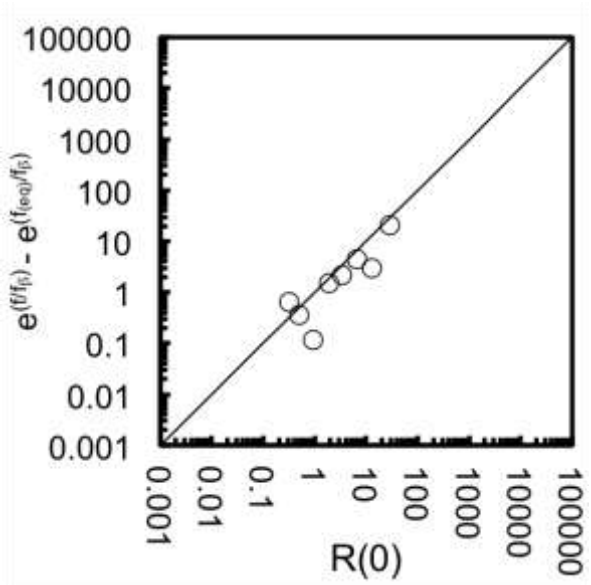

Figure S5. Plot of the same data shown in figure 4(a) in the main text plotted in the natural coordinates of equation S1, showing the collapse of the data onto a straight line.

References

[S1] A. Janshoff, M. Neitzert, Y. Obersörfer, and H. Fuchs, *Angew. Chem. Int. Ed.,* 2000, **39**, 3212.
[S2] F. Oesterhelt, M. Rief, and H. E. Gaub, *New Journal of Physics* 1999, **1**, 6.
[S3] S. Guo, N. Li, N. Lad, S. Desai, and B. B. Akhremitchev, *Journal of Physical Chemistry C*, 2010, **114**, 8755.
[S4] R. W. Friddle, A. Noy, and J. J. De Yoreo, *PNAS*, 2012, **109**, 13573.
[S5] A. Noy, and R. W. Friddle, *Methods*, 2013, **60**, 142.